Dalton Transactions

COMMUNICATION

View Article Online
View Journal

Cite this: DOI: 10.1039/c7dt03689b

Received 1st October 2017,
Accepted 29th November 2017

DOI: 10.1039/c7dt03689b

rsc.li/dalton

Addition of azomethine ylides to carbon-encapsulated iron nanoparticles†

Artur Kasprzak, *[a] Anna M. Nowicka,[b] Jakub P. Sek,[b] Maciej Fronczak,[b] Michał Bystrzejewski,[b] Mariola Koszytkowska-Stawinska[a] and Magdalena Poplawska[a]

The Prato reaction was applied for the covalent introduction of a variety of organic moieties onto carbon-encapsulated iron nanoparticles. The developed method is versatile and employs a broad range of commercially available reactants, including both aromatic and aliphatic aldehydes. The reported functionalization route provides high functionalization yields (*ca.* 12–21 wt%).

The cycloaddition reaction is one of the most commonly used synthetic routes to functionalize carbon nanostructures for various applications. Since the discovery of fullerenes in 1985 a number of their possible modifications have been developed, including the cycloaddition protocols.[1–3] Over the years, it has been found that such a methodology can also be applied for the surface modification of carbon nanotubes[4–6] and graphene.[7–9] Graphene, in principal, has a flat structure and does not contain topological defects which introduce the local curvature and in consequence its reactivity is lower in comparison with fullerenes and carbon nanotubes. Such a phenomenon influences the reaction conditions for the functionalization of graphene, especially higher temperatures and longer reaction times are needed. Nevertheless, there are a number of cycloaddition reactions possible to conduct with the graphene layer. Many examples were recently summarized by Prato and co-workers.[10]

Carbon-encapsulated magnetic nanoparticles constitute as a family of carbon nanostructures. They comprise a magnetic core which is covered by curved graphene layers.[11,12] The carbon shell protects the metallic core against environmental factors, *e.g.* oxidation and aggregation/agglomeration. Carbon-encapsulated magnetic nanoparticles possess a wide range of possible applications, including *e.g.* adsorption,[13–15a] sensors[15b] and nanomedicine.[16–18] Several types of radical reactions with the exterior graphene layer of carbon-encapsulated magnetic nanoparticles have been established to date, including diazo[13] and peroxide chemistry,[19] as well as the direct amination protocol.[20] These functionalization routes constitute as a direct link to the chemistry of fullerenes[21,22] and carbon nanotubes.[23,24] Importantly, the addition of nitrile oxides to carbon-encapsulated magnetic nanoparticles can also be conducted.[25] If so, one can conclude that this magnetic graphene-related material can act as an active dipolarophile in the cycloaddition reaction like other carbon allotropes.

The Prato reaction is one of the most popular methods to functionalize carbon nanostructures. It is based on the 1,3-cycloaddition of azomethine ylides generated from the corresponding amino acids and aldehydes. The leading role of this reaction in the modification of carbon allotropes results from (i) effortless of the manual operation, (ii) employing commercially available reactants and (iii) providing high functionalization yields. The Prato reaction has been reported for fullerenes,[27] carbon nanotubes,[28] as well as for graphene.[29] To the best of our knowledge the addition of azomethine ylides to the carbon-encapsulated magnetic nanoparticles has not been reported yet. In this paper, we report the syntheses of new derivatives of carbon-encapsulated iron nanoparticles (CEINs) using the Prato reaction. It is shown that various types of functional moieties can be efficiently introduced onto the surface of CEINs by employing the developed process.

The carbon arc discharge route was employed to obtain CEINs, which have a diameter between 10 and 100 nm.[30] The magnetic core has a diameter of 10–30 nm, whilst the carbon shell is composed of *ca.* 5–20 graphene layers. The developed functionalization route (Fig. 1) involved refluxing CEINs (20 mg) with aldehydes (1.0 mmol) in the presence of sarcosine (0.8 mmol). The toluene or toluene/DMSO (1 : 1) system was used as the reaction medium. For experimental details see the ESI.† The mass gain was observed for each material. However, this feature only indicates the success of the reaction, because CEINs-based materials are highly hygroscopic. Fourier-transform infrared (FT-IR) spectroscopy and thermogravimetry (TGA) were performed to confirm the success of functionalization.

[a]Faculty of Chemistry, Warsaw University of Technology, Noakowskiego Str. 3, 00-664 Warsaw, Poland. E-mail: akasprzak@ch.pw.edu.pl
[b]Faculty of Chemistry, University of Warsaw, Pasteura Str. 1, 02-093 Warsaw, Poland

†Electronic supplementary information (ESI) available: Experimental details; TGA, FT-IR and NMR data; electrochemical measurements. See DOI: 10.1039/c7dt03689b

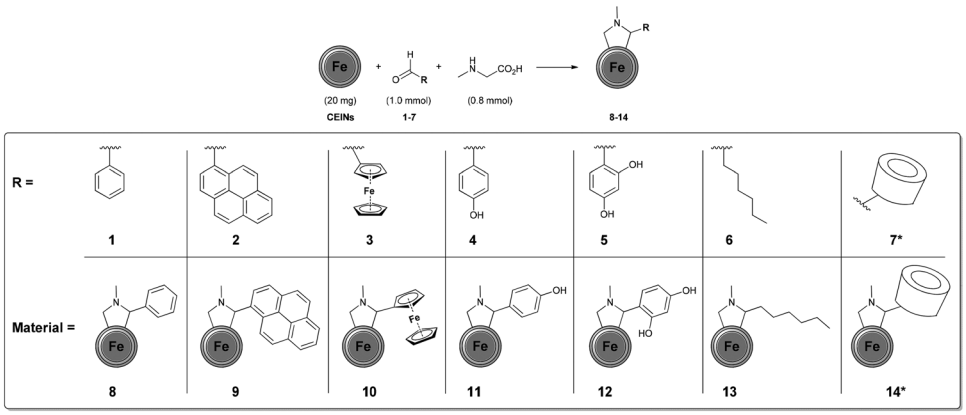

* for the chemical structure of β-cyclodextrin, see Fig. S1 in ESI

Fig. 1 The developed method for the functionalization of CEINs. *For the chemical structure of β-cyclodextrin, see Fig. S1 in the ESI.†

FT-IR spectroscopy provided qualitative information about the structure of the obtained materials. Firstly, the non-substituted aromatic aldehydes (**1**–**2**) were attached to the CEINs surface. The FT-IR spectrum of the representative material **9** is presented in Fig. 2 (for the spectrum of material **8** see Fig. S7 in the ESI†). The FT-IR spectrum of pristine CEINs is also shown. The weak absorption band at 1585 cm^{-1} is observed in the FT-IR spectrum of pristine CEINs only. In contrast, the spectra of the obtained materials consist of several strong absorption bands. As for example, the main features for material **9** are located at 1585, 1510, 1460, 1390, 1270, 1155, 960, 820, 685, and 460 cm^{-1}. The characteristic absorption bands at 1585, 820, 685, and 640 cm^{-1} were assigned to the C=C stretching and out-of-plane deformation vibrations. The adsorption bands at 1510, 1460, 1390, 1270, 1155, and 960 cm^{-1} were assigned to the vibrations of the *N*-methylpyrrolidine ring (C–N vibrations associated with the presence of the tertiary amine group as well as C–C vibrations). Importantly, no characteristic absorption band for the aldehyde group of the starting reactant (*ca.* 1730–1670 cm^{-1}; see data in section S5.2 in the ESI†) was observed. This finding supports the conclusion that the organic moieties were covalently attached to CEINs. Obviously, the substituted *N*-methylpyrrolidine ring is formed on the surface of the functionalized CEINs.

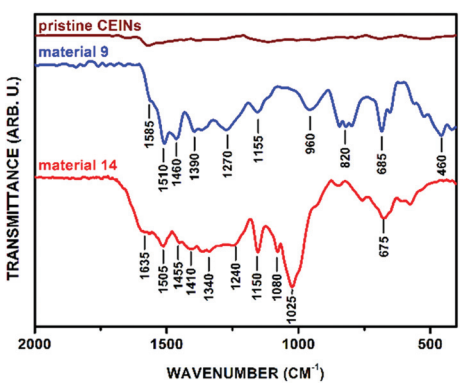

Fig. 2 FT-IR spectra of pristine CEINs, material **9** and material **14**. For legends, see Fig. 1.

The success of such preliminary studies prompted us to broaden up the range of the aldehydes employed in the reported process. Ferrocenecarboxaldehyde (**3**) was chosen as the representative metallocene compound. The covalent attachment of the ferrocene (Fc) moiety was confirmed by FT-IR spectroscopy (material **10**, Fig. S8 in the ESI†). The attachment of the aromatic moieties substituted with hydroxyl groups, namely 4-hydroxybenzaldehyde (**4**) and 2,4-dihydroxybenzaldehyde (**5**), was also achieved (FT-IR spectra of materials **11** and **12** are presented in Fig. S9 and S10 in the ESI,† respectively). The addition reactions with the hydroxyl-substituted aldehydes were conducted in the DMSO/toluene solvent system. Subsequently, heptanal (**6**) was applied as the representative aliphatic aldehyde. Once again, FT-IR spectroscopy was performed to confirm the success of the covalent attachment of the aliphatic moiety. The characteristic absorption bands for both the ligand and *N*-methylpyrrolidine ring were found in the spectrum of the material **13** (Fig. S11 in the ESI†). The addition of the azomethine ylide generated from the β-cyclodextrin aldehyde (βCD-CHO, **7**)[31] to the surface of CEINs was also succeeded. The characteristic strong absorption bands resulting from βCD (especially C–O–C vibrations arising from the glucose units, *i.e.* 1080 and 1025 cm^{-1}) and the *N*-methylpyrrolidine ring were found in the FT-IR spectrum of the obtained carbon material (**14**, Fig. 2). No characteristic absorption band for the aldehyde group of βCD-CHO (C=O, 1720 cm^{-1}, Fig. S6 in the ESI†) was observed.

The content of the introduced organic moieties was calculated from the thermogravimetric (TGA) curves. The representative TGA curves (acquired in nitrogen) of materials **9** and **14** are presented in Fig. 3 (for other TGA curves see Fig. S13–S17 in the ESI†). The TGA curve for pristine CEINs is also shown. The first weight loss is observed between *ca.* 65 and 105 °C for both pristine CEINs and the corresponding materials. It is

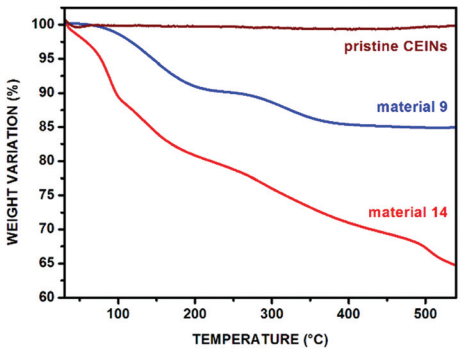

Fig. 3 TGA curve (in nitrogen) of pristine CEINs, materials **9** and **14**. For legends, see Fig. 1.

associated with the presence of moisture in the samples. The next weight loss up to 550 °C is observed only for the materials **8–14** and is directly attributed to the thermal decomposition of the introduced moieties. This temperature range is typical of the decomposition of covalently attached moieties to CEINs.[20,26,32] The functionalization yields ranging from 12 wt% to 21 wt% are summarized in Table 1. The details of the calculation are presented in the ESI (section S6†). The highest content of the introduced moiety was found for material **10** bearing the Fc unit (21.2%) and material **14** bearing the βCD moiety (20.8%).

To exclude a possible non-covalent adsorption of organic moieties onto CEINs, the representative organic aldehydes **2**, **3** and **5** (1.0 mmol) were refluxed with CEINs (20 mg) in the absence of sarcosine. As expected, the lack of sarcosine, the crucial reaction component for the formation of the intermediate ylide, prevented the covalent functionalization of CEINs. No weight gain was observed. Moreover, no characteristic absorption bands for the aldehydes in the FT-IR spectra were observed. Furthermore, no weight loss in the TGA curves of the obtained carbon materials was observed (data presented in section S7 in the ESI†). These findings revealed that the studied organic compounds were not permanently adsorbed onto the CEINs. Consequently, our thesis on the covalent modification of CEINs in the course of the developed functionalization route was supported.

Carbon nanomaterial **10** with the Fc unit was expected to show an interesting electroactivity. To explore its electrochemical properties and to determine the potential range of electroactivity, nanomaterial **10** was physically adsorbed on the glassy carbon electrode and subjected to the cyclic voltammetry experiments in the range of positive potentials. Both well-defined one anodic peak and one cathodic peak are observed in the cyclic voltammogram as presented in Fig. 4. These peaks confirm the successful conjugation of Fc residues to CEINs. The shift of the current signals on the potential scale in comparison with the unsubstituted ferrocene[33] is a consequence of the interactions between the electron-donating ligand and the cyclopentadienyl ring. The calculated amount of Fc constituted *ca.* 18 wt% of the total weight of the carbon material **10** adsorbed at the electrode surface. This number is in very good agreement with the TGA data (*ca.* 21 wt%). It means that almost all Fc residues attached to the CEINs surface are capable of electron exchange with the electrode. The detailed electrochemical characteristic of the carbon material **10** is presented in section S8, ESI.†

βCD is a well-known host molecule that participates in the formation of the supramolecular host–guest systems.[34,35] Hence, the immobilization of β-cyclodextrin (βCD) onto CEINs (material **14**) gives a possibility to bind hydrophobic chemical molecules to the functionalized carbon material. In particular, the interactions between βCD and Fc are of significant interest because of the high Fc@βCD association constant and the reversibility of the inclusion. When Fc is oxidized to an ferrocenium cation (Fc^+) no complex with βCD is formed.[36,37] We have examined the possibility of complexing the Fc inside the CEINs–βCD material and the subsequent release of Fc^+ using the oxidizer. Importantly, after complexation of Fc inside βCD in material **14**, Fc could be released from the complex (material **15**) using the aqueous solution of iron(III) chloride (Fig. 5a, for experimental details see section S3.4 and discussion in section S5.3 in the ESI†). This process is visualized in Fig. 5b–d. When material **14** was sonicated in an aqueous solution of $FeCl_3{\cdot}6H_2O$ and then centrifuged, no color change of the supernatant was observed in comparison with $FeCl_{3aq}$ (Fig. 5b and c). In contrast, when material **15** was subjected to the same experiment, the color of the supernatant changed (Fig. 5d). This difference was associated with the oxidation of Fc to Fc^+ followed by its release from the complex.

Table 1 Content of the introduced moieties (evaluated from TGA). See Fig. 1 for legends

Material no.	Content of introduced moiety [wt%]	Material no.	Content of introduced moiety [wt%]
8	11.8	**12**	18.2
9	13.3	**13**	12.0
10	21.2	**14**	20.8
11	17.0		

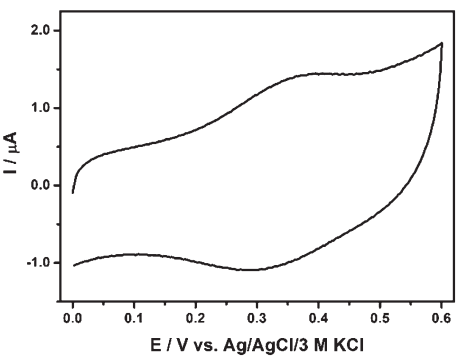

Fig. 4 Cyclic voltammograms of material **10** adsorbed on the glassy carbon surface in 0.02 M PB buffer containing 0.15 M K_2SO_4, pH 7.40. Experimental conditions: T = 21 °C; scan rate 100 mV s^{-1}; ⌀ GC 3 mm. For legend, see Fig. 1.

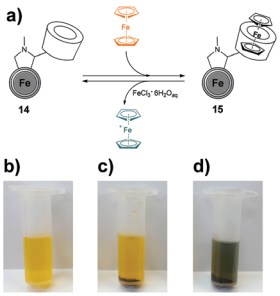

Fig. 5 Complexation tests with Fc: (a) reaction scheme, (b) aqueous solution of $FeCl_3{\cdot}6H_2O$ (20 mg mL^{-1}), (c) material **14** after treatment with $FeCl_3{\cdot}6H_2O_{aq}$, (d) material **15** after treatment with $FeCl_3{\cdot}6H_2O_{aq}$. See the description in the text.

Conclusions

We have succeeded in the covalent functionalization of carbon-encapsulated iron nanoparticles (CEINs) *via* the addition of azomethine ylides. The developed method is a one-step process and employs commercially available reactants. Both aromatic and aliphatic aldehydes, as well as metallocene and sugar aldehydes were used in the developed process. The presented functionalization approach enables one to functionalize CEINs both with small organic ligands and unique supramolecules (cyclodextrin). The content of the introduced organic moiety was between 12 and 21%. For material **10** bearing the ferrocene unit, the characteristic electrochemical signals were highly consistent with the data for the ferrocene compound. This is a first example of the ferrocene–CEINs conjugate with well-defined electrochemical performance. Material **14** containing β-cyclodextrin units exhibited interesting complexation features, which have been proven by demonstrating the reversible host–guest interactions between β-cyclodextrin and ferrocene. In other words, the characteristic properties of the organic moieties were retained after covalent immobilization onto CEINs. The developed functionalization route opens up a way to modify magnetic carbon-related materials for a variety of applications.

Conflicts of interest

There are no conflicts to declare.

Acknowledgements

This work was financially supported partially by the National Science Center (Poland) through the Grant PRELUDIUM No. 2016/21/N/ST5/00864 and the Warsaw University of Technology.

Notes and references

1 M. Prato, *J. Mater. Chem.*, 1997, 7, 1097–1109.
2 J.-F. Nierengarten, *New J. Chem.*, 2004, 1177–1191.
3 N. Zydziak, B. Yameen and C. Barner-Kowollik, *Polym. Chem.*, 2013, **4**, 4072.
4 D. Tasis, N. Tagmatarchis, A. Bianco and M. Prato, *Chem. Rev.*, 2006, **106**, 1105–1136.
5 P. Singh, S. Campidelli, S. Giordani, D. Bonifazi, A. Bianco and M. Prato, *Chem. Soc. Rev.*, 2009, **38**, 2214.
6 M. Alvaro, P. Atienzar, P. De La Cruz, J. L. Delgado, V. Troiani, H. Garcia, F. Langa, A. Palkar and L. Echegoyen, *J. Am. Chem. Soc.*, 2006, **128**, 6626–6635.
7 A. Hirsch, J. M. Englert and F. Hauke, *Acc. Chem. Res.*, 2013, **46**, 87–96.
8 S. Sarkar, E. Bekyarova, S. Niyogi and R. C. Haddon, *J. Am. Chem. Soc.*, 2011, **133**, 3324–3327.
9 J. Li, M. Li, L. L. Zhou, S. Y. Lang, H. Y. Lu, D. Wang, C. F. Chen and L. J. Wan, *J. Am. Chem. Soc.*, 2016, **138**, 7448–7451.
10 M. Quintana, E. Vazquez and M. Prato, *Acc. Chem. Res.*, 2013, **46**, 138–148.
11 M. Bystrzejewski, A. Huczko and H. Lange, *Sens. Actuators, B*, 2005, **109**, 81–85.
12 G. Wang, G. Wan and C. Hao, *Mod. Phys. Lett. B*, 2009, **23**, 2149–2153.
13 R. N. Grass, E. K. Athanassiou and W. J. Stark, *Angew. Chem., Int. Ed.*, 2007, **46**, 4909–4912.
14 P. Strachowski and M. Bystrzejewski, *Colloids Surf., A*, 2015, **467**, 113–123.
15 (*a*) R. Fuhrer, I. K. Herrmann, E. K. Athanassiou, R. N. Grass and W. J. Stark, *Langmuir*, 2011, **27**, 1924–1929; (*b*) E. Matysiak, M. Donten, A. Kowalczyk, M. Bystrzejewski, I. P. Grudzinski and A. M. Nowicka, *Biosens. Bioelectron.*, 2015, **64**, 554–559.
16 I. P. Grudzinski, M. Bystrzejewski, M. A. Cywinska, A. Kosmider, M. Poplawska, A. Cieszanowski and A. Ostrowska, *J. Nanopart. Res.*, 2013, **16**, 1835.
17 G. Modugno, C. Ménard-Moyon, M. Prato and A. Bianco, *Br. J. Pharmacol.*, 2015, **172**, 975–991.
18 J. K. Park, J. Jung, P. Subramaniam, B. P. Shah, C. Kim, J. K. Lee, J. H. Cho, C. Lee and K. B. Lee, *Small*, 2011, **7**, 1647–1652.
19 M. Poplawska, M. Bystrzejewski, I. P. Grudzinski, M. A. Cywinska, J. Ostapko and A. Cieszanowski, *Carbon*, 2014, **74**, 180–194.
20 A. Kasprzak, M. Poplawska, M. Bystrzejewski and I. P. Grudzinski, *J. Mater. Chem. B*, 2016, **4**, 5593–5607.
21 G. P. Miller, *C. R. Chim.*, 2006, **9**, 952–959.
22 X. Ma and Y. Zhao, *Chem. Rev.*, 2015, **115**, 7794–7835.
23 E. V. Basiuk, M. Monroy-Peláez, I. Puente-Lee and V. A. Basiuk, *Nano Lett.*, 2004, **4**, 863–866.
24 Y. Ying, R. K. Saini, F. Liang, A. K. Sadana and W. E. Billups, *Org. Lett.*, 2003, 1471–1473.
25 M. Poplawska, G. Z. Zukowska, S. Cudziło and M. Bystrzejewski, *Carbon*, 2010, **48**, 1318–1320.
26 A. Kasprzak, M. Bystrzejewski, M. Koszytkowska-Stawinska and M. Poplawska, *Green Chem.*, 2017, **19**, 3510.
27 M. Maggini, G. Scorrano and M. Prato, *J. Am. Chem. Soc.*, 1993, **115**, 9798–9799.

28 J. J. Mulvey, E. N. Feinberg, S. Alidori, M. R. McDevitt, D. A. Heller and D. A. Scheinberg, *Int. J. Nanomed.*, 2014, **9**, 4245–4255.
29 M. Quintana, K. Spyrou, M. Grzelczak, W. R. Browne, P. Rudolf and M. Prato, *ACS Nano*, 2010, **4**, 3527–3533.
30 M. Bystrzejewski, O. Łabedź, W. Kaszuwara, A. Huczko and H. Lange, *Powder Technol.*, 2013, **246**, 70–15.
31 M. J. Cornwell, J. B. Huff and C. Bieniarz, *Tetrahedron Lett.*, 1995, **36**, 8371–8374.
32 A. Kasprzak, M. Poplawska, M. Bystrzejewski, O. Labedz and I. P. Grudzinski, *RSC Adv.*, 2015, **5**, 85556–85567.
33 N. G. Tsierkezos, *J. Solution Chem.*, 2007, **36**, 289–302.
34 J. Szejtli, *Chem. Rev.*, 1998, **98**, 1743–1753.
35 G. Crini, *Chem. Rev.*, 2014, **114**, 10940–10975.
36 A. Harada and S. Takahashi, *J. Chem. Soc., Chem. Commun.*, 1984, 645.
37 M. Nakahata, Y. Takashima, H. Yamaguchi and A. Harada, *Nat. Commun.*, 2011, **2**, 511.